SPECIAL TOPIC — International Conference on Nanoscience & Technology, China 2013

Properties of passive nano films on zircaloy-4 affected by defects induced by hydrogen permeation*

Gu Jun-Ji(顾俊骥)[a], Ling Yun-Han(凌云汉)[a]†, Zhang Rui-Qian(张瑞谦)[b], Dai Xun(戴 训)[b], and Bai Xin-De(白新德)[a]

[a] School of Materials Science and Engineering, Tsinghua University, Beijing 100084, China
[b] Reactor Fuel and Materials Laboratory, Nuclear Power Institute of China, Chengdu 610041, China

(Received 4 September 2013; revised manuscript received 10 January 2014; published online 10 June 2014)

In this work, hydrogen absorption and the permeation behavior of the passive layer formed on zircaloy-4 are investigated. Potentiodynamic polarization, Mott–Schottky analysis, electrochemical impedance spectroscopy, and Raman scattering spectroscopy are employed to characterize the passive defects before and after hydrogen permeation. It is found that the nanoscale passive ZrO_2 films play an important role in the resistance against corrosion; hydrogen impingement, however, reduces the passive impedance towards hydrothermal oxidation. The increase of defects (vacancies) in passive film is probably attributed to the degradation. We believe that this finding will provide valuable insight into the understanding of the corrosion mechanism of zircaloys used in light water reactors.

Keywords: zircaloy, defects, hydrogen permeation, electrochemical measurement

PACS: 81.07.–b, 82.45.–h, 82.45.Bb, 68.47.Gh **DOI:** 10.1088/1674-1056/23/8/088106

1. Introduction

Zircaloys are widely used as the cladding materials for light water reactors (LWRs). They present good mechanical properties and workabilities, and have remarkable corrosion resistances.[1] The latest tendencies toward high fuel burn-up, extended recycle and high pH operation for increasing energy efficiency have led to the need to improve the corrosion resistance of zircaloy-4 cladding.[2] In recent years, hydrogen behavior in nuclear fuel cladding attracted researchers' attention for the reason that the working life of the fuel cladding is dependent on the oxidation of zirconium alloys due to hydrogen absorption through the oxide film.[3] The reaction with cooling water on the surface of the fuel cladding causes the oxidation of the cladding and the release of hydrogen subsequently. Some fraction of the released hydrogen is picked-up and diffuses into the zircaloy matrix, which results in the formation of hydrogen precipitates.[4] The hydrogen that is absorbed by zircaloy-4 cladding in a pressurized water reactor (PWR) after high fuel burn-up becomes one of the factors that limit the achievable working life of the fuel.[5,6]

The passive ZrO_2 film plays a key role in resisting corrosion and acting as an effective barrier against hydrogen permeation. A protective oxide layer is mainly composed of a mixture of tetragonal and monoclinic ZrO_2, which is conducible to resisting hydrogen diffusion through the oxide layer in which the O–H bonds exist.[7] It is believed that dense passive ZrO_2 films with as few defects as possible are essential for effective protection against hydrogen permeation, about which, however, little knowledge has been obtained because of the difficulties in detecting the hydrogen.

Hydrogen permeation is an electrochemically credible method used to investigate the behavior of hydrogen diffusing through an oxide layer by applying a hydrogen concentration gradient. Many researches have been performed using this method to study the effects of defect (vacancy) and surface condition on the permeation behavior in various metal–hydrogen systems.[8,9] However, the research on the hydrogen behavior in zircaloy using this method for cladding materials is still scant. In the present study, the properties of two kinds of passive ZrO_2 films prepared by hydrothermal oxidation and vacuum oxidation under various conditions (before and after hydrogen permeation) are investigated. The microstructures, defects, and surface conditions before and after hydrogen permeation are compared.

2. Experiment

2.1. Sample preparation

Zircaloy-4 (Zr-4) with dimensions of ϕ8.2 mm × 1.6 mm was chosen in this experiment. Some pretreatments were carried out to flatten and clean the surface before oxidation. Details are given in Table 1.

*Project supported by the National Basic Research Program of China (Grant No. 2011CB610501), the Funds from the State Key Laboratory of Surface and Chemistry, China (Grant No. SPC 201102), and the Reactor Fuel and Materials Laboratory, China (Grant No. STRFML-2013-05).

†Corresponding author. E-mail: yhling@mail.tsinghua.edu.cn

© 2014 Chinese Physical Society and IOP Publishing Ltd

Table 1. Details of the pretreatment of Zr-4.

Number	Process	Time	Concrete operation
1	polishing	–	polishing with 200#∼2000#SiC waterproof abrasive paper
2	cleaning	30 minutes	ultrasonic cleaning in acetone
3	cleaning	30 minutes	ultrasonic cleaning in ethanol
4	cleaning	–	cleaning with deionized water three times
5	drying and storing	–	preserving in vessels after drying

2.2. Passive film formation

Vacuum oxidation and hydrothermal oxidation were employed to form passive films on zircaloy-4. For vacuum oxidation, samples were placed in a tube furnace to be heated in a vacuum atmosphere (about 1 kPa); while for hydrothermal oxidation, samples were placed in an autoclave with aqueous solutions containing 0.1-M H_3BO_3 + 0.001-M LiOH to simulate the PWR primary water chemistry. The detailed conditions are listed in Table 2.

2.3. Hydrogen permeation

The electrochemical hydrogen permeation tests were performed in the aqueous solutions containing 0.1-M H_3BO_3 + 0.001-M LiOH. A constant cathodal current density, 0.5 mA/cm^2, was applied to the Zr-4-containing passive ZrO_2 film for 30 min at a charge quantity of about 0.5 C.

2.4. Electrochemical tests

The samples covered with passive films before and after hydrogen permeation were made into electrodes for the use of electrochemical tests. The open circuit potential (OCP) was first measured for 2 h until the value was stable. After that, the electrochemical impedance spectroscopy (EIS) test was performed using an excitation voltage of 10 mV (peak-to-peak) and an applied frequency from 1 MHz to 0.01 Hz. Potentiodynamic polarization curves were recorded using a voltage scan rate of 0.1667 mV/s from a point 0.1 V more negative than the OCP to a point 0.1 V more positive than the OCP. Mott–Schottky curves were measured by the capacitance with an excitation voltage of 10 mV (peak-to-peak) at a frequency of 1 kHz. Besides, cyclic voltammetry curves were also recorded from 0 V to 50 mV.

2.5. Microstructural characterization

Raman scattering spectroscopy tests were performed to compare the microstructures of the passive ZrO_2 films prepared on the surface of zircaloy-4 before permeation and those after hydrogen permeation.

3. Results and discussion

3.1. Thickness of passive ZrO_2 film

The steady state film thickness, L_{ss} is estimated by the well-known 'parallel plate' expression for the capacitance

$$L_{ss} = \frac{\varepsilon\varepsilon_0}{C}. \quad (1)$$

The interfacial capacitance C is obtained from $C = -1/\omega Z''$.[10] The thickness values of the passive ZrO_2 films are displayed in Table 2 together with the OCP values of the films.

Table 2. Thickness and OCP values of the passive ZrO_2 films.

Method of oxidation	Temperature/°C	Time/h	Thickness of films/nm	OCP values/mV
Vacuum	350	2	143.4	250
Vacuum	350	5	189.7	79
Vacuum	350	8	234.1	43
Hydrothermal	100	24	29.4	187
Hydrothermal	150	24	33.7	210
Hydrothermal	200	24	54.2	250

One can see from Table 2 that the OCP value of the film prepared by vacuum oxidation decreases with the increase of the thickness of the film while the OCP value increases as the film becomes thicker for the hydrothermally oxidized one, which shows that as the film oxidized in vacuum becomes thicker, more defects exist in the film, thereby degrading the performance of the nanoscale passive ZrO_2 film.

3.2. Electrochemical impedance spectroscopy

Electrochemical impedance spectra (EISs) for the passive ZrO_2 films are recorded over a wide frequency range from 1 MHz to 0.01 Hz. The EIS data may be plotted in two ways: Nyquist plots (complex plane) and Bode plots. A Nyquist plot is the plot of Z'' versus Z', i.e., the imaginary part versus the real component for various frequencies. The other is the Bode plot, i.e., $\log|Z|$ (magnitude) and phase angle, ϕ, versus $\log f$. The Nyquist plot allows for an easy prediction of

the circuit elements and a distinct identification of conduction process present, while the Bode plot contains all the necessary information.[10]

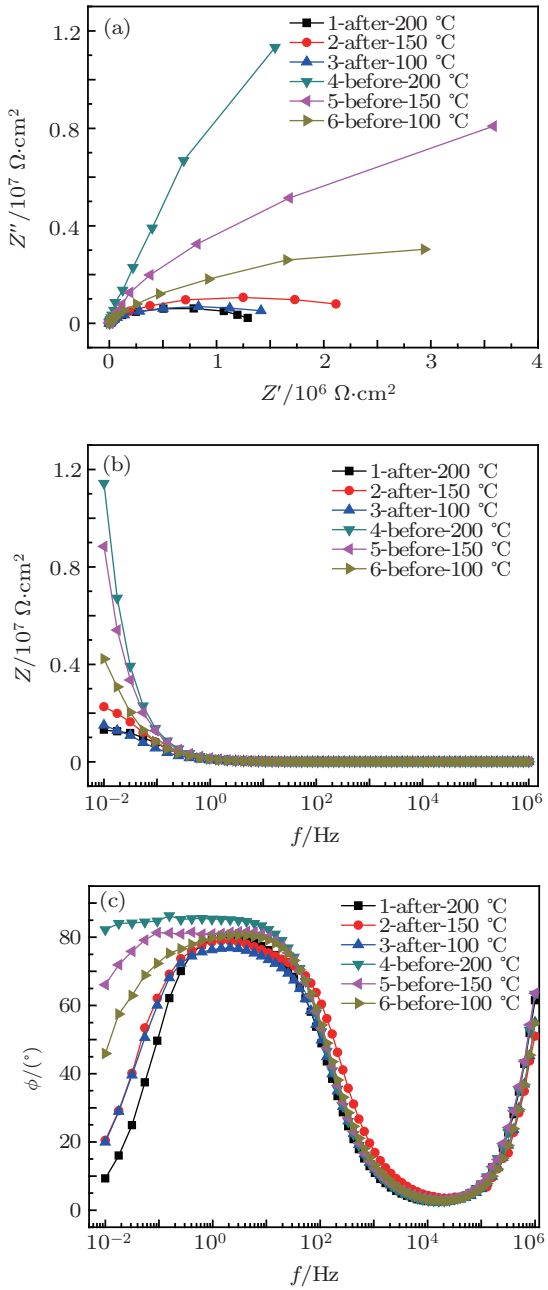


Fig. 1. (color online) Nyquist (a) and Bode ((b) and (c)) plots for zircaloy-4 oxidized hydrothermally.

Figure 1 shows Nyquist and Bode plots for zircaloy-4 oxidized hydrothermally in the 0.1-M H_3BO_3 + 0.001-M LiOH solution. With the increase of heating temperature, the passive films become thicker and the magnitude of the impedance of the nanoscale passive films become higher. After hydrogen permeation, the value of the impedance decreases and the phase angle drops off obviously at low frequencies. Figure 2 shows Nyquist and Bode plots for zircaloy-4 oxidized in vacuum in the same aqueous solution as the above. On the contrary, the value of the impedance increases after hydrogen permeation. Figure 3 reveals the plots for the blank zircaloy. The magnitude of the impedance of the hydrogenated zircaloy is much higher than that of the blank zircaloy. It might be that hydrogen penetrates into the zircaloy and forms zirconium hydride, which leads to the increase in impedance. Besides, we can infer that the hydrogen penetrates through the nanoscale passive film prepared by vacuum oxidation which has more defects and is easier for hydrogen to diffuse than the one prepared by hydrothermal oxidation into the zircaloy matrix, and then results in the increase in impedance, while hydrogen mainly penetrates into the passive film oxidized hydrothermally and gives rise to numerous vacancies, which is reflected through the decrease of impedance.

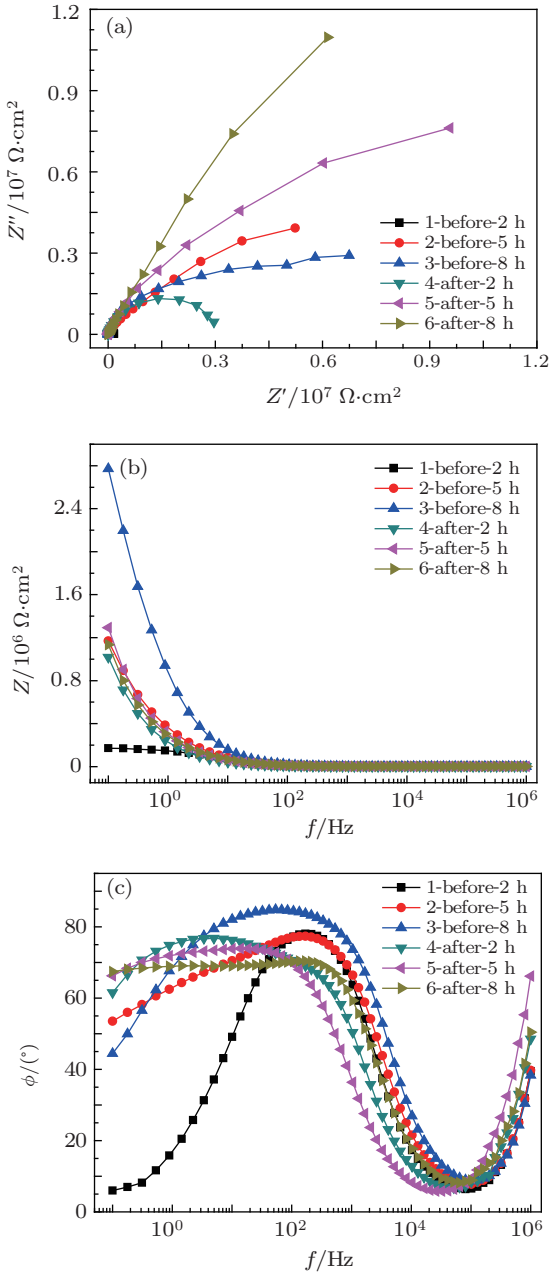


Fig. 2. (color online) Nyquist (a) and Bode ((b) and (c)) plots for zircaloy-4 oxidized in vacuum.

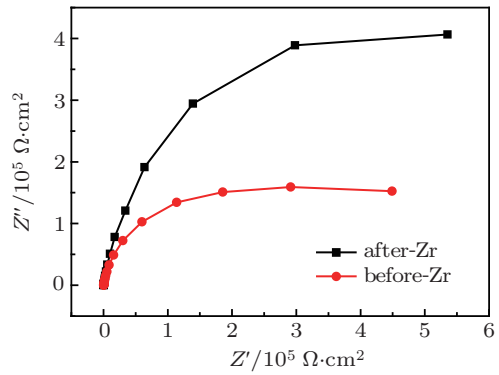


Fig. 3. (color online) Nyquist plots for the zircaloy-4.

3.3. Polarization

Under potentiodynamic conditions, the logarithm of the current is measured as a function of the electrode potential by starting the voltage sweep at a rate of 1 mV/s from a point 0.1 V more negative than the OCP to a point 0.1 V more positive than the OCP (Fig. 4). The self-corrosion potential of the passive film prepared by hydrothermal oxidation increases as heating temperature rises. After hydrogen permeation, both the self-corrosion potential and the self-corrosion current increase. For the film oxidized in vacuum, there is no apparent changing tendency, which may be due to the thickness and defects of the passive film, both of which affect hydrogen permeation through the passive film.

3.4. Mott–Schottky analysis

According to the Mott–Schottky theory, C_{sc} (F/cm^2), the space charge capacitances of n-type and p-type semiconductor junctions are given by

$$\frac{1}{C_{sc}^2} = \frac{2}{\varepsilon\varepsilon_0 q N_D}\left(V - V_{fb} - \frac{kT}{q}\right), \quad \text{n-type}, \tag{2}$$

$$\frac{1}{C_{sc}^2} = \frac{-2}{\varepsilon\varepsilon_0 q N_A}\left(V - V_{fb} - \frac{kT}{q}\right), \quad \text{p-type}, \tag{3}$$

respectively.[12]

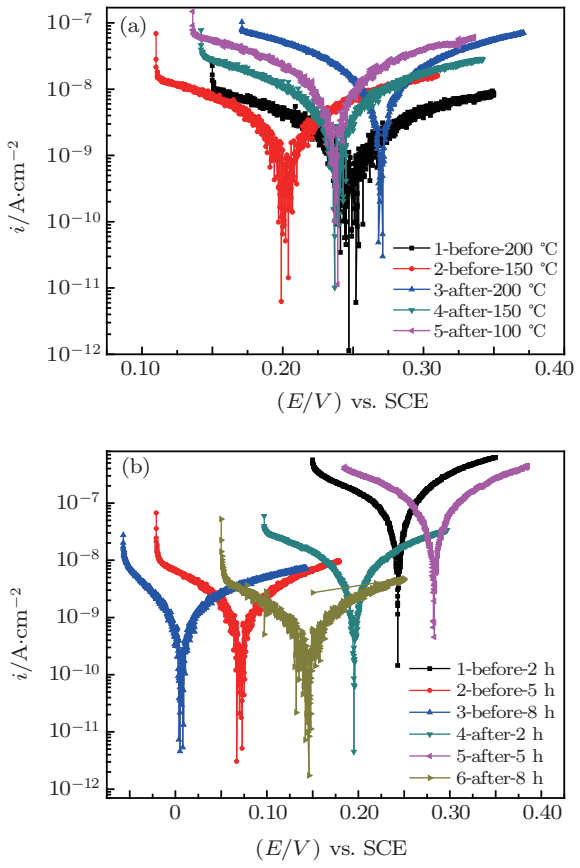


Fig. 4. (color online) Polarization curves of passive films before and after hydrogen permeation for (a) hydrothermal oxidation and (b) vacuum oxidation.

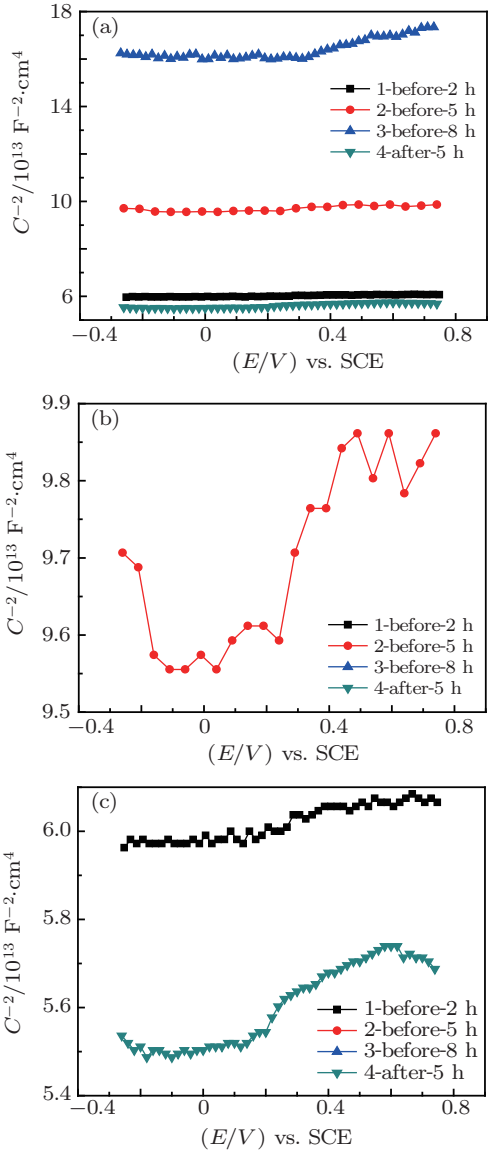


Fig. 5. (color online) (a) Mott–Schottky curves for vacuum oxidized passive films before and after hydrogen permeation; (b) and (c) figures of partial enlargement.

Figure 5 shows the Mott–Schottky curves recorded in the experiment. From the slope of the linear region, all the passive films prepared in this experiment can be determined to be of an n-type semiconductor and then the donor concentration can be calculated through the value of slope. The results are shown in Fig. 6.

With the oxidation time of passive film increasing, the donor concentration decreases, which means fewer oxygen vacancies. After hydrogen permeation, the donor concentration increases obviously. It can be inferred that the penetration of hydrogen causes more oxygen vacancies.

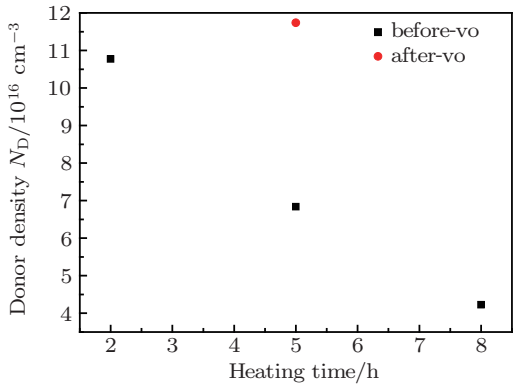


Fig. 6. (color online) Donor density N_D of the passive film formed on Zr-4 as a function of heating time by vacuum oxidation before and after hydrogen permeation.

3.5. Cyclic voltammetry

The surface characteristics of ZrO_2 nanoscale passive film can be evaluated by the double layer capacitive change of the electrode/electrolyte interface without illumination.[13] Figures 7(a)–7(c) each show a typical voltammetric pattern at different scan rates for passive films before and after hydrogen permeation. The I–V curves are measured at scan rates ranging from 0.5 mV/s to 9 mV/s. At each sweep rate, the charging current is recorded in the middle of the scan range and is plotted as a function of the sweep rate. It appears that the current is linearly dependent on the sweep rate and the intercepts are negative (Fig. 7(d)). From the slope, the capacitance of the nanoscale passive ZrO_2 film/electrolyte interface, i.e.,

$$C_{\rm dl} = {\rm d}q/{\rm d}E = {\rm d}j/{\rm d}v)$$

is estimated. The capacitance of the film prepared by vacuum oxidation for 5 h before hydrogen permeation is 14.4 μF/cm^2 while the value becomes negative after hydrogen permeation, which means that the surface capacitance of the film decreases after hydrogen permeation. It might be caused by the hydrogen penetrating into the film and forming some zirconium hydride, which needs further investigation.

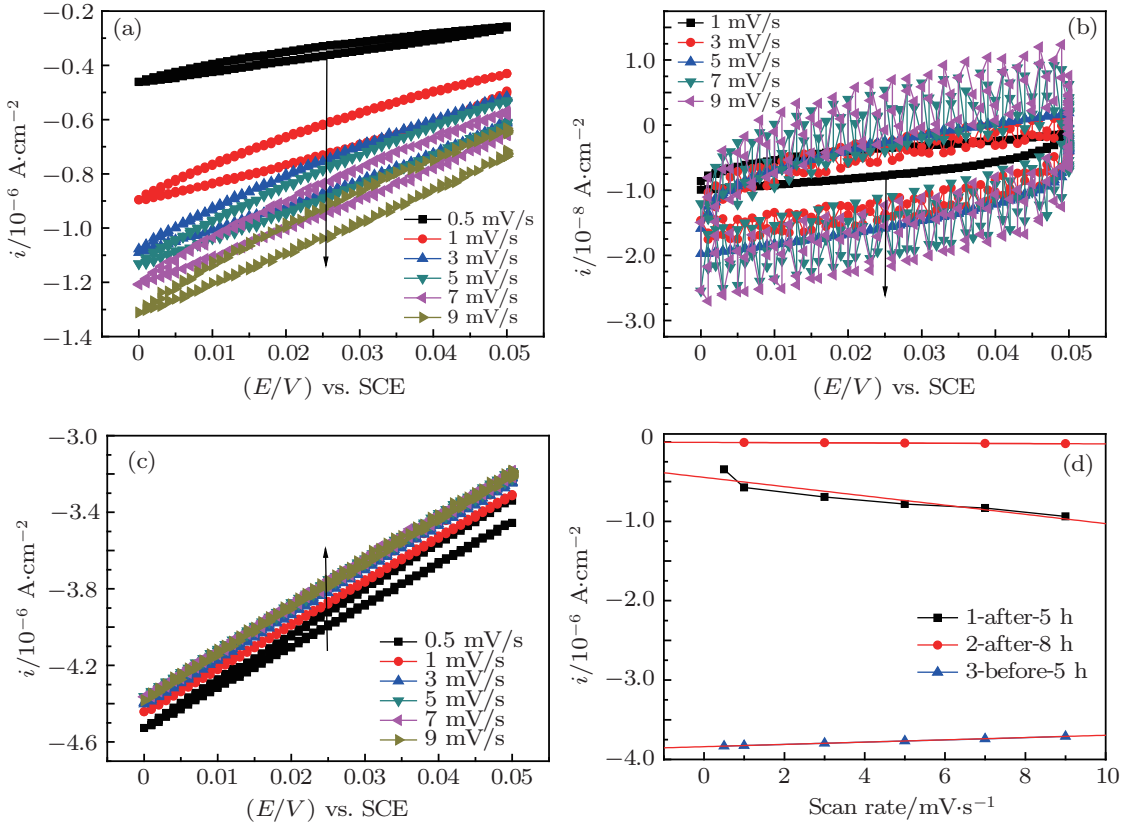


Fig. 7. (color online) Interface capacitive characteristics of ZrO_2 passive films. (a)–(c) Cyclic voltammograms in the double-layer region of the films vacuum oxidized for 5 h and 8 h after hydrogen permeation and the film oxidized for 5 h before hydrogen permeation respectively; (d) Charging current as a function of scan rate.

3.6. Raman scattering spectra

The Raman scattering spectra of ZrO_2 nanoscale passive films are shown in Fig. 8. The results all present three main peaks, which are located at 176 cm^{-1}, 477 cm^{-1}, and 636 cm^{-1} respectively, which is in good agreement with those of the baddeleyite. Other small peaks also accord with the data of the baddeleyite while the main peaks of the tetragonal ZrO_2, at 266 cm^{-1} and 644 cm^{-1}, measured in Ref. [14] are not found in the spectrogram. Thus, the nanoscale passive ZrO_2 films in our work are predominantly monoclinic.

It is also observed that the intensities of the peaks of the films after hydrogen permeation are apparently lower than before permeation, which means that the hydrogen permeation results in non-crystallizing, which might be due to the fact that hydrogen penetrates into the passive films and thus causes more defects, oxygen vacancies.

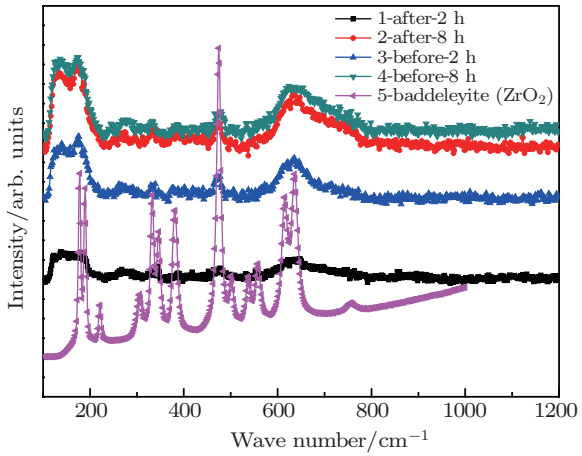


Fig. 8. (color online) Comparisons of the Raman scattering spectrum of ZrO_2 nanoscale passive films prepared by vacuum oxidation, before and after hydrogen permeation.

4. Conclusions

Two kinds of passive films formed on Zr-4 are investigated. From the results some conclusions can be drawn below.

(i) Both the passive films formed by hydrothermal and vacuum oxidation are of the nanoscale ranging from 29.4 nm to 234.1 nm, and the magnitudes of impedance of the films prepared by the same method of oxidation turn higher as the thickness values of the passive films become larger. After hydrogen permeation, the impedance values of the films oxidized in vacuum increase while those of the films oxidized hydrothermally decrease.

(ii) For potentiodynamic polarization, the self-corrosion potential of the passive film prepared by hydrothermal oxidation increases as heating temperature rises. After hydrogen permeation, both the self-corrosion potential and the self-corrosion current increase.

(iii) With increasing the oxidation time of passive films, the donor concentration i.e., the density of oxygen vacancies, decreases. After hydrogen permeation, the donor concentration increases obviously, which might be hydrogen penetrating into the passive films and causing a great deal of defects as indicated by the Mott–Schottky analysis and the Raman scattering spectra.

References

[1] Khatamian D 1997 *J. Alloys Compd.* **253** 471
[2] Cox B 1997 *J. Alloys Compd.* **256** 244
[3] Elmoselhi M B 1995 *J. Alloys Compd.* **231** 716
[4] Lim B H, Hong H S and Lee K S 2003 *J. Nucl. Mater.* **312** 134
[5] Guedeney P, Trotabas M, Boschiero M, Forat C and Blanpain P 1991 *Proceedings of the International Topical Meeting on LWR Fuel Performance* (Avignon: Academy of Natural Sciences) p. 141
[6] Vesterlund G and Corsetti L V 1994 *Proceedings* 1994 *International Topical Meeting on Light Water Reactor Fuel Performance* (Florida: Academy of Natural Sciences) p. 17
[7] Zieliński A and Sobieszczyk S 2011 *Int. J. Hydrogen Energy* **36** 8619
[8] Brass A M and Chanfreau A 1996 *Acta Mater.* **44** 3823
[9] Manolatos P, Jerome M, Duret-Thual C and Le Coze J 1995 *Corros. Sci.* **37** 1773
[10] Chen Y, Urquidi-Macdonald M and Macdonald D D 2006 *J. Nucl. Mater.* **348** 133
[11] Macdonald J R 1992 *Ann. Biomed. Eng.* **20** 289
[12] Macdonald D D 1992 *J. Electrochem. Soc.* **139** 3434
[13] Ling Y, Liao J, Liu X, *et al*. 2010 *J. Nanosci. Nanotechnol.* **10** 7020
[14] Barberis P, Merle-Méjean T and Quintard P 1997 *J. Nucl. Mater.* **246** 232